International Journal for Multidisciplinary Research (IJFMR)
E-ISSN: 2582-2160 ● Website: www.ijfmr.com ● Email: editor@ijfmr.com

Cost-Effective Fabrication of c-Si Solar Cell Using Transition Metal Oxides Interfaces

Bhoora Ram[1], Shrikant Verma[2]

[1]Research Scholar, Department of Physics, Poornima University, Jaipur, India.
[2]Associate Professor, Department of Physics, Poornima University, Jaipur, India.

Abstract

For global energy supply and demand to be reached, non-traditional energy sources like photovoltaic (PV) technology are crucial. With a market share of 95% and an efficiency range of 20 to 25%, crystalline solar cells (c-Si) based on aluminium back surface (Al-B.S.F.) and passivated emitter and rear contact (P.E.R.C.) exhibit efficiency levels of 20% and 25%, respectively. The SHJ solar cells have passivation of i:a-si:H and doped a-Si:H, enabling 26.7% efficiency; however, the fabrication process is complicated for doped a-Si:H contacts and emits hazardous gases, and energy losses from parasitic absorption and Auger recombination are still present. Transition metal oxides (TMOs) contacts as an alternate can be fabricated at low temperatures and have more economical, opto-electrical, and other properties that can reduce energy losses. TMOs act as carrier-selective contacts, allowing one kind of charge carrier to pass while obstructing the other. TMOs with double-asymmetric heterocontact with an efficiency of 24.83% have been attained by c-Si solar cells and a potential of above 28.4%. By adjusting TMOs deposition thickness, assessing passivation quality, and measuring V_{oc}, I_{sc}, and FF using a solar simulator with Keithley, the I-V measurement, and different spectroscopy, it is possible to experimentally choose the TMOs material and tune it with c-Si for good passivation. By reducing manufacturing costs and establishing a levelized cost of energy (LCOE), solar power becomes more competitive and economically viable.

Keywords: Crystalline Silicon Solar cell, Transition Metal Oxide (TMO), Passivated Contacts, Cost-Effective , Interface, Carrier Selectivity.

1. Introduction

Photovoltaic technology (PV) has been the dominant competitor for decades due to its sustainable and reliable nature, 95% market share, and longer stability (Wang Y. et al., 2023; Ballif et al., 2022). Doping of hydrogen with a-Si is used in commercial solar cells; these amorphous silicon layers are carrier-selective but emit hazardous gases during the doping process, and for safety purposes, it increases the thermal budget (Zeng Y et al., 2022). Another barrier to improving PV device performance is that both p- and n-type hydrogenated amorphous silicon have a small energy band gap. Due to their intrinsic defect states and energy loss by parasitic absorption and Auger recombination, they emit toxic and flammable fumes that damage the environment and are expensive (Liu et al., 2020; Wang Y et al., 2023). SHJ technology, consisting of a doped a-Si:H coating for contact creation, has the highest efficiency of 26.7% with interdigitated back contact (IBC) (Masmitja G. et al., 2018), which is less than the theoretical maximum limit of 29.43% (Shockley W. et al., 2018). It can be replaced with hole- and electron-

selective molybdenum trioxide (MoO_3) and titanium oxide (TiO_2) of transition metal oxide (TMO) to reduce parasitic absorption and energy band offset issues (Koswatta P. et al., 2015; Masmitja G. et al., 2022; Mehmood H. et al., 2020).

TMOs are affordable, readily accessible, have a wide range of job functions, and have the advantage of being optical and easily depositionable on silicon wafers.Many transition metal oxides have carrier selectivity due to their altering work function, which causes an oxygen vacancy in the metal.TMOs can be hole- or electron-selective, depending on the cations or metallic vacancies. Large work functions, such as MoO3, WO3, and V2O5, easily align with the silicon surface's valence band. A low-valence band offset hole can travel through while electrons are inhibited at the interface. Because of their low work function and electron affinity, TiO_2, ZnO, Nb_2O_5, and other materials operate as electron-selective contacts. Metal oxide's conduction band coincides with the silicon energy band, resulting in a low conduction band offset that allows electrons to flow while blocking holes with a broad valence band offset.

SiO_2 acts as a passivation, inducing band bending while preserving the electric field for tunnelling charge carriers.When trivalently doped with hydrogenated amorphous silicon, it is hole-selective, where as pentavalently doped with hydrogenated amorphous silicon is electron-selective. When a-Si:H is p-doped and replaced with MoO_3, the solar cell reaches 22.5% efficiency (Bullock J et al., 2019).TiO2 replaces n-doped a-Si:H in a SHJ solar cell, resulting in a 21.2% efficiency (Cao Y. et al., 2020).When both doped a-Si:H connections in the SHJ solar cell are replaced by TMOs contacts, the maximum efficiency of 23.5% is attained, with an additional potential of 28.4% (Dréon J. et al., 2020; Michel J. Ibarra et al., 2023).Through simulation, it was observed that the efficiency was up to 24.83%, employing MoO_3 and TiO_2 as hole and electron selective contacts with thicknesses of 07 nm and 5 nm, respectively, and SiO_2 as a passivation layer with a thickness of roughly 1 nm (Mehmood H. et al., 2020) and a potential of more than 28.4% (Michel J. Ibarra, et al., 2023; Imran H. et al., 2016).

Using TMO contacts, the performance of the c-Si solar may be enhanced with interdigitated back contact architecture technology (Allen TG. et al., 2019). If it is possible to experimentally choose the TMO material and tune it with c-Si for good passivation, solar power becomes more competitive and economically viable (Battaglia C, et al., 2016 ; Wong T.K.S. et al., 2022 ; García-Hernansanz R. et al., 2023).

2. Fabrication of Experimental Cell

The novel design and configuration of a solar cell are shown in Figure 1.

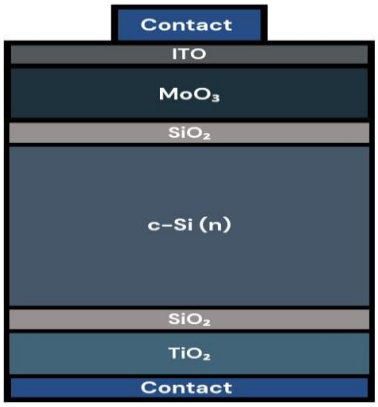

Figure 1: Novel Design of TMO Contact c-Si Solar Cell.

The novel solar cell utilizes titanium oxide as an electron-picking contact and MoO_3 as a hole-selective contact. Silicon wafers of n-type, Czochralski, or floating zone are used, and R.C.A. I and R.C.A. II solutions in 2% HF are used for cleaning the wafer (Patwardhan S. et al., 2018). Thermal evaporation, or

atomic layer deposition (ALD) or pulse laser deposition (PLD), is used to grow the MoO_3 film on one side while the TiO_2 film is grown on the other (Kumari J. et al., 2020). SiO_2 is deposited on both sides of a thickness around 1.2 nm, or the SiO_2 layer is inherently present on a silicon wafer of thickness 1 to 2 nm after cleaning by RCA I and RCA II when not dipping in HF (Lin H et al., 2023). ITO serves as an anti-reflection coating on the front surface of the MoO_3 layer, with Ag deposited at the front and Al deposited at the rear surface (Sagar R. et al., 2020). The Si wafer is kept within the chamber during thermal evaporation for TiO_2 deposition. Tetrakis dimethyleamido titanium and water steam are employed as precursors for titanium and oxygen, respectively, at temperatures < 200 °C (Yu C. et al., 2018). Ozone and $Mo(CO)_6$ are used as precursors for Mo and oxygen deposition of MoO_3 films on Si wafers. The pressure in the chamber remained constant at 1 Torr throughout the experiment. MoO_3 films are grown to a thickness of 7 nm, TiO2 is 5 nm, and ITO is RF sputtered to a thickness of 80 nm at ~200 °C (Sanyal S. et al., 2019). 300 nm Ag is evaporated to metalize the device's front using a shadow mask with a bus-bar and finger pattern. Solar devices utilize silver and aluminium contacts for anode and cathode electrodes, respectively, with a single ITO antireflection coating at the top interface for efficient solar energy production (Mehmood H. et al., 2020; Patwardhan S. et al., 2018).

3. Experiment with Two Different Configuration of Devices

Device 1: MoO3 thin film deposited on the front of the Si wafer (without passivation), as hole-selective contact with an ITO coating as an anti-reflection coating (ARC), and above that, a silver coating with a bus bar pattern on the front, while Al is coated on the back surface of the silicon wafer, as shown in the upper part of figure 2 (Dhar A et al., 2020). The energy band diagram is shown in figure 2.

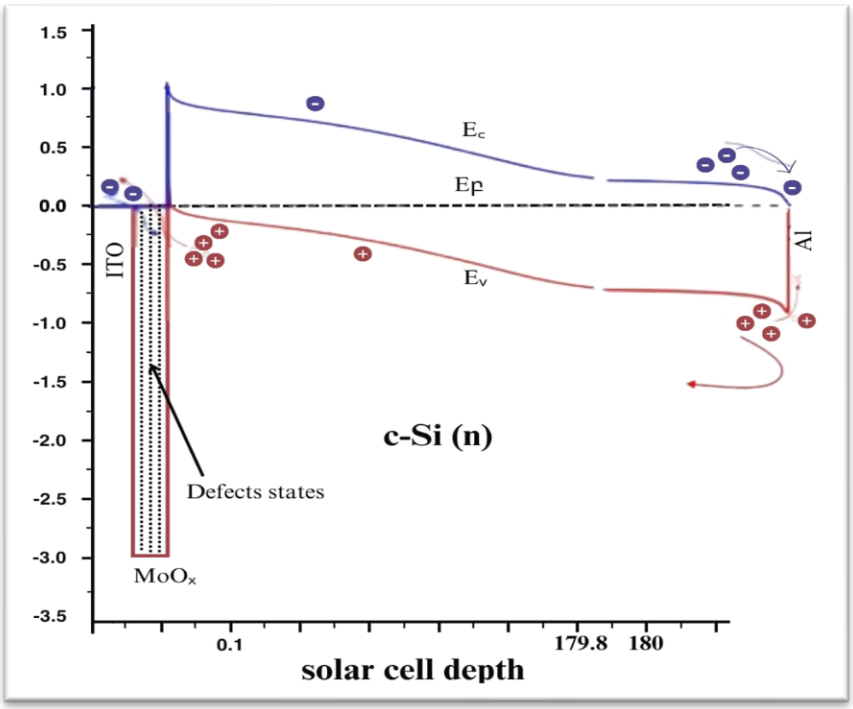

Figure 2: Energy Band Diagram Analysis of Devices 1

MoO_3's high work function of 6.9 eV aligns the Fermi level closer to the valence band of the c-Si absorber, creating a wide Schottky barrier and a narrow barrier for electrons and holes so that the holes collected at the anode terminal and electrons at the cathode. Molybdenum oxide work function depends upon the number of O_2 vacancies within the TMO layer (Mehmood H. et al., 2019). If the number of ox-

ygen vacancies increases, then work function will be less due to the increasing number of defect levels, and the donor level is nearing the conducting band (C.B.). A solar cell with a configuration of MoOx/cSi (where x represents the oxygen vacancies) has the performance of a device with varying thicknesses (5 nm, 7 nm, 10 nm, and 15 nm) of MoO_x with the Si wafer, and the efficiency is achieved at 14.05%, 18.69%, 16.56%, and 13.21%, respectively. It was found that a MoO_3 thickness of 7 nm with a Si wafer achieved an efficiency of 18.69%, which is the maximum due to its good passivation with The silicon surface generates a greater electrical field. At a thickness greater than 15 nm, both the fill factor and efficiency are reduced due to increased defect volume, parasitic absorption, increasing recombination losses, and the potential barrier height for holes (Mehmood H. et al., 2020).

Device 2: It is device 1 with SiO_2 passivation in which both sides of the polished n-type silicon wafer on one side, MoO_3, and on the rear side, TiO_2, are deposited by thermal evaporator/atomic layer deposition or pulse laser deposition (Messmer et al., 2018). On the molybdenum trioxide surface, ITO coating of around 80 nm is done, as is silver coating for anti-reflection coating, and on the back surface, Al coating is both around 200 nm. The energy band diagram as shown in figure 3 of solar device-2, in which the SiO_2 passivation layer is 1.2 nm and TMO asymmetric heterocontact MoO_3 as hole-picking and TiO_2 as electron-picking contact to increase the electron potential barrier by more than 5 eV, Electrons are blocked at the upper interface and tunnel into ultra-thin SiO_2 at the back for collection at the negative electrode, while holes are directed towards the anode (Plakhotnyuk MM , et al., 2017 ; Mehmood H., et al., 2020).

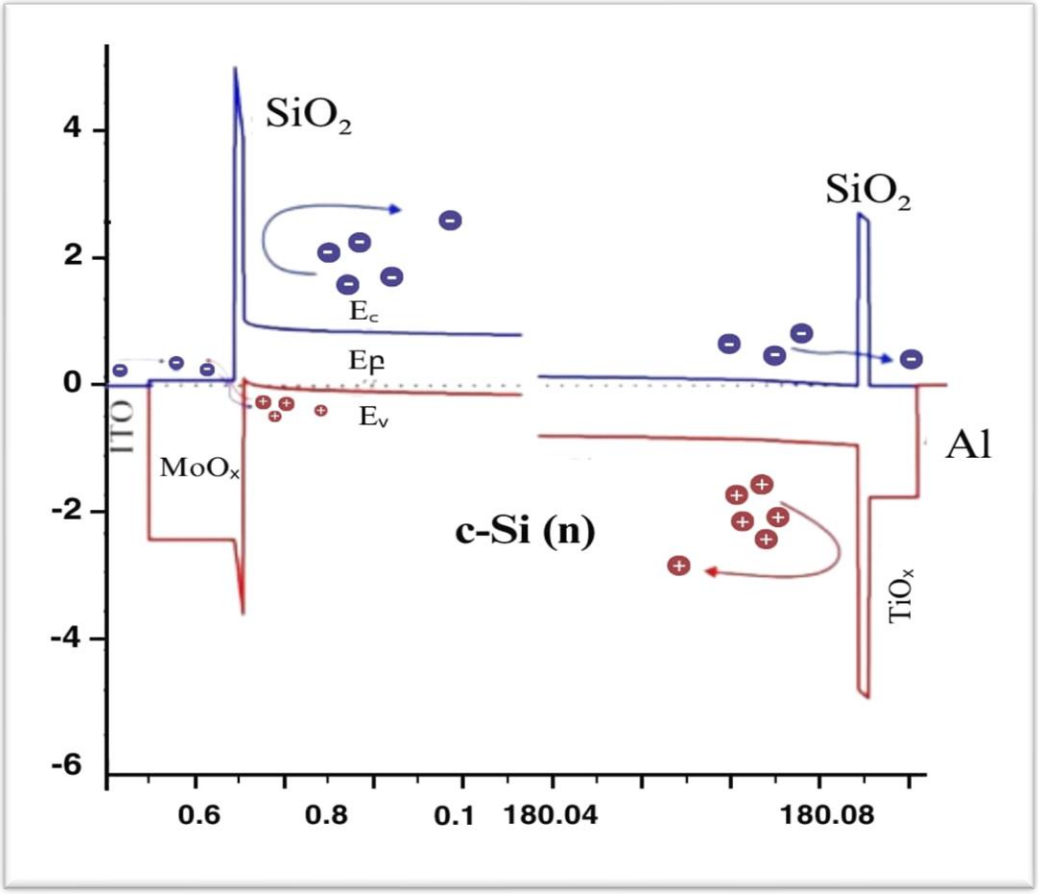

Figure 3: Energy Band Diagram Analysis of Devices 2.

Further optimization of hole and electron selective contact with c-Si data can help find the appropriate combination of electron and hole carrier selective contacts (Messmer et al**.,** 2018)**.**TMO asymmetric het-

erocontact solar cells can achieve efficiencies of MoO3 as hole-picking and TiO2 as electron-picking contact of around 23.5% (García-Hernansanz R, et al., 2023), while TMO double-asymmetric heterocontact/passivated contacts with a SiO2 passivation layer of 1 nm and c-Si solar cells have an efficiency of 24.83%. and a further potential of more than 28.4% (Yoshikawa K, et al., 2017; Michel J. Ibarra, et al., 2023). The next step should be to optimize current carrier-elective substances and contact architectures by employing novel contact and interfacial passivation substances, cost-effective deposition processes, and unique device designs, including fully back-contact (Almora et al., 2017; Michel J. Ibarra et al., 2023).

4. Variation of Efficiency with Work-Function of MoO_x

The work function of molybdenum oxide depends upon the number of O_2 vacancies; when vacancies increase, the work function will be less due to the increasing number of defect levels, and the donor level is nearing the conduction band (C.B.). (Melskens J. et al., 2018). The effect of the work function of MoO_x on the energy band diagram is that with a low work function of 4.5 eV, the energy band stays practically flat. Incorporating SiO_2 with a c-Si absorber causes band bending with the valence band of c-Si. More holes will be able to pass the insulator barrier by tunneling, in contrast to the growing barrier that those holes must encounter with low-function MoO_x (Liu Y. et al., 2021 Z Zhao Y. et al., 2023).

The effective hole barrier's height at the SiO_2/c-Si interface was reduced from 5.5 to 3.5 eV, increasing the chance of hole tunnelling through SiO_2 while also increasing electric field strength. MoO_x with a very thin layer can thus allow the conveyance of tunneled holes, thereby enhancing the photovoltaic endurance of the device (Martín I, et al., 2023). The maximum simulated open-circuit of 785 mV was reached with a MoO_x work function of 6.9 eV, resulting in a productivity of 24.83% for the doping-free asymmetric heterocontact device employing SiO_2 as the passivation layer so far (Wu W, et al., 2018; Kang D, et al., 2023). The band bends significantly for SiO2, corresponding to an increased electric field intensity of more than 109 V/m, as illustrated in Figure 4.

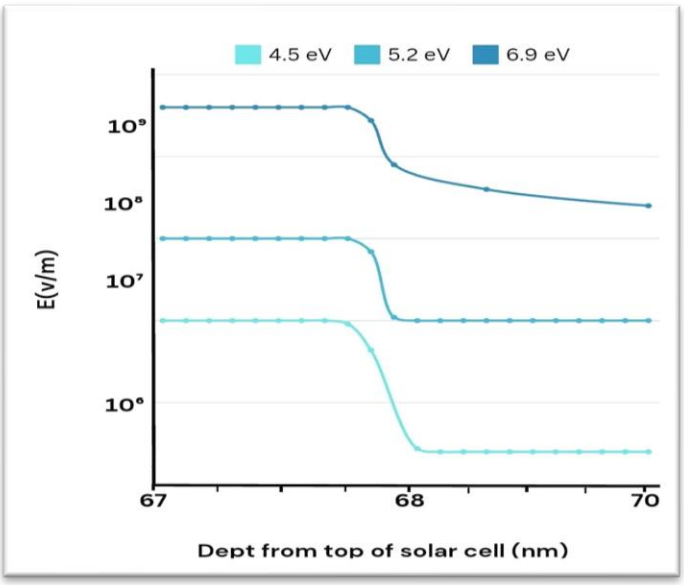

Figure 4: Graph Plotted Between Electric Field and Work function

Hence, for doping free asymmetric heterocontact solar cells employing SiO_2 as passivation layers, deploying MoOx with a greater work function improves the charge transportation properties of PV devices (Nagamatsu K.A. et al., 2018; Schmidt J. et al., 2018).

5. Variation of Efficiency with Thickness of Passivation Layer.

The wideness of SiO_2 as a passivation coating is an important parameter that determines The J-V features associated with solar cells are presented in Figure 5.

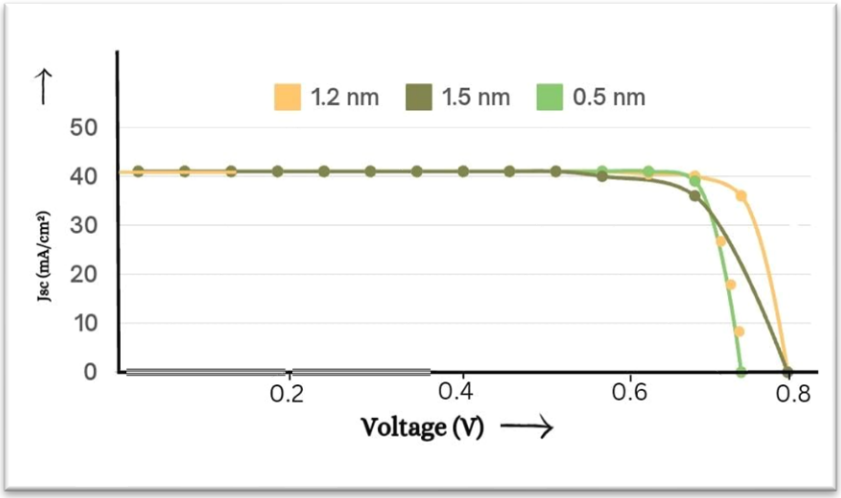

Figure:5 J-V Graph with Different Thicknesses of SiO2

In Figure 5, better performance is found with a SiO_2 thickness of around 1 nanometer. When the wideness of SiO_2 increases, the J_{sc} or (I_{sc}/A) decreases due to the recombination of carriers, and the fill factor of the device decreases with a wideness greater than 1.2 nanometers. Device -2, featuring around 1 nm SiO_2, exhibited a Voc of 785 millivolts, a Jsc of 41.0 milliamperes/cm^2, a fill factor of 77.00%, and η of 24.83% by simulation (Mehmood H. et al., 2020). The fill factor and Jsc of Device-2 were slightly reduced to 77% and 41.0 milliamperes/cm^2 due to defects within SiO_2 contributing to low recombination whenever the charge carriers are tunneling (Liu Y. et al., 2021). The recombination aspect may not lower the photovoltaic performance of the device for a lower value of contact resistivity (ρ_c) and interface defect states (Dit), The work-function of MoO_3 has been optimized to 6.9 eV and approximately 4.0 eV for TiO_2, a voc of more than 780 millivolts, an efficiency of 24.83%, and a potential of more than 28.4% (Green M. et al., 2022). Device-2 facilitates the deposit of TMOs with carrier-selective interfaces and SiO_2 coatings with a reduced thermal budget (Michel J. Ibarra et al., 2023).

6. Result and Discussion

Device -1 (MoO_x/c-Si), the performance of a device with varying thicknesses (5 nm, 7 nm, 10 nm, and 15 nm) of MoO_x with the Si wafer, and the efficiency are achieved at 14.05%, 18.69%, 16.56%, and 13.21%, respectively (Yang X et al., 2016). It was found that a MoO_3 thickness of 7 nm with a Si wafer achieved an efficiency of 18.69%, which is the maximum due to its good passivation with the c-Si surface, which results in a greater electric field. At a thickness greater than 15 nm, both the fill factor and efficiency are reduced due to increased defect volume, parasitic absorption, increasing recombination losses, and the potential barrier height for holes. TMO asymmetric heterocontact solar cells can achieve efficiencies of MoO3 as hole-picking and TiO2 as electron-picking contact of around 23.5% (Yan D. et al., 2018; Markose K.K. et al., 2020).

Device-2 TiO_2 and MoO_3 as electron and hole selective contacts, with SiO_2 as the passivation layer, a novel c-Si solar cell consists of molybdenum oxide and titanium oxide as hole- and electron-choosing interfaces with a passivation of 1 nm. SiO_2 enhanced the energy barrier height up to ~5 eV by inserting stacks of SiO_2/TiO_2 (Liu Y. et al., 2021). The higher work function of molybdenum oxide induced sig-

nificant band distorting at the front, while TiO_2, which has low electron affinity, decreased the potential barrier on rear contacts. Contact-specific resistance of around 10 milli-Ohm cm and a wideness of 7 nanometers for MoO_3, TiO_2 of 5 nm, and inserting the SiO_2 layer with MoO_3 elevated the band bending, which reduced the hole barrier height. The thickness of 1 nm SiO_2 helps in tunnelling the majority of charge carriers through it (Ritcher A. et al., 2021). impressive V_{oc} of 785.00 milli-volt, J_{sc} of 41.0 milli-ampere/cm^2, fill factor of 77.00%, efficiency of 24.830%, and a further potential of more than 28.4% (Michel J. Ibarra et al., 2023). A solar cell made of SiO_2 as a passivation layer and incorporating MoO_3 and TiO_2 as holes as well as electron-selective contacts is abundant in nature and cost-effective (Parashar PK et al., 2021). It improves the potential barrier against minority carriers with increased band bending at both interfaces and increasing efficiency up to 24.83% (Michel J. Ibarra et al., 2023). Device 2 is treated as a next-generation SHJ structure using transition metal oxide carrier-choosing contacts and passivation by SiO_2. It reduces the thermal budget and can be used commercially (Wong T.K.S. et al., 2022).

7. Conclusion

c-Si is the leading photovoltaic technology, having a 95% share of the market worldwide and having a longer stability of more than 20 years. For the performance improvement of c-Si solar cells, it is crucial to focus on improving their passivation and efficiency. The efficiency of SHJ c-Si solar cells is currently at 26.7%, with significant improvements due to passivated contacts of doped a-Si, which damage the environment and are expensive. The carrier-selective TMO passivated contacts are essential for reducing recombination and parastic absorption. In this article, we present a novel fabrication of solar cells with TMO contacts (TiO_2 and MoO_3) as electron and hole-selective contacts as an alternative to doped a-Si:H contacts, which is cost-effective and eco-friendly. Different thickenings of MoO_3 are used, and we find that at 7 nm, TiO_2 at 5 nm, and a SiO_2 passivation layer of 1.2 nm best optimizes, with the silicon surface and achieves an efficiency of 24.83%. By adopting an interdigitated back contact (IBC) structure with SHJ-based transition metal oxide contact, the efficiency can be improved, and this technology has a potential of more than 28.4%. TMO passivated contacts for c-Si solar cells, which have generated interest and the potential to lower the manufacturing expenses and, as a result, provide a levelized cost of energy (LCOE) to our society with eco-friendliness in the era of global warming.

References

1. Acharyya S., Sadhukhan S., Panda T., Ghosh DK., Mandal NC., Nandi A., Bose S., Das G., Maity S., Chaudhuri P., and Saha H. “Dopant-free materials for carrier-selective passivating contact solar cells”: A review. Surfaces and Interfaces. 2022 Feb 1;28:101687.https://doi.org/10.1016/j.surfin.2021.101687
2. Allen TG., Bullock J., Yang X., Javey A., and Wolf D.S., “Passivating contacts for crystalline silicon solar cells." Nature Energy. 2019 Nov, 4(11):914-28. DOI 10.1038/s41560-019-0463-6
3. Almora O., Gerling LG., Voz C., “Alcubilla R., Puigdollers J., Garcia-Belmonte G. Superior performance of V2O5 as hole-selective contact over other transition metal oxides in silicon heterojunction solar cells”. Solar Energy Materials and Solar Cells, 2017 Aug 1, 168:221-6. http://hdl.handle.net/2117/104004
4. Avasthil S., Nagamatsu K. A., Jhaveril J., McClainl W. E., Manl G., Kahn A., Schwartzl J., Wagner S., Sturml J. C., “Double-heterojunction crystalline silicon solar sell fabricated at 250°C with 12.9%

efficiency", IEEE, October 2014, 40, 949–953. **DOI:** 10.1109/PVSC.2014.6925069
5. Ballif C., Haug FJ., Boccard M., Verlinden PJ., and Hahn G., "Status and perspectives of crystalline silicon photovoltaics in research and industry." Nature Reviews Materials, 2022 Aug;7(8):597-616. https://doi.org/10.1038/s41578-022-00423-2
6. Battaglia C., Cuevas A., and Wolf S.D., "High-efficiency crystalline silicon solar cells: status and perspectives." Energy and Environment Science,. February 2016, 9, 1552–1576, DOI: 10.1039/c5ee03380b
7. Bullock J., Y. Wan Y., Xu Z., S. Essig S., Hettick M., Wang H., W. Ji, Boccard M., Cuevas A., Ballif C., A. Javey A., "Stable dopant-free asymmetric heterocontacts: Silicon solar cell efficiencies above 20%", ACS Energy Letter, March 2018, 3(3), 508–529, DOI 10.1021/acsenergylett.7b01279
8. Bivour M., Zähringer F., Ndione P., and Hermle M., "Sputter-deposited WOx and MoOx for hole selective contacts." Energy Procedia. 2017 Sep 1;124:400–5. doi:10.1016/j.egypro.2017.09.259.
9. Bullock J., Wan Y., Hettick M., Zhaoran X., Phang S.P., Yan D., Wang H., Ji W., Samundsett C., Hameiri Z., Macdonald D., "Dopant-free partial rear contacts enabling 23% silicon solar cells. Advanced Energy Materials". 2019 Mar, 9(9):1803367.doi:10.1002/aenm.201803367
10. Bullock J., Hettick M., Geissbühler J., Ong AJ., Allen T., Sutter-Fella CM., Chen T., Ota H., Schaler EW., Wolf D.S., Ballif C., "Efficient silicon solar cells with dopant-free asymmetric heterocontacts." Nature Energy. 2016 Jan 25, 1(3):1-7.doi:10.1038/nenergy.2015.31
11. Cao Y., Shengzhi X., "Recent Advances in and New Perspectives on Crystalline Silicon Solar Cells with Carrier-Selective Passivation Contacts," Crystals, November 2018, 8,430–447. https://doi.org/10.3390/cryst8110430
12. Chee KW., Ghosh BK., Saad I., Hong Y., Xia QH., Gao P., Ye J., and Ding ZJ., "Recent advancements in carrier-selective contacts for high-efficiency crystalline silicon solar cells: an industrially evolving approach." Nano Energy, 2022, May 1, 95:106899. https://doi.org/10.1016/j.nanoen.2021.106899
13. Dhar A., Ahmad G., Pradhan D., and Roy J.N., "Performance analysis of a c-Si heterojunction solar cell with passivated transition metal oxide carrier-selective contacts." Journal of Computational Electronics. 2020 Jun;19:875-83. https://doi.org/10.1007/s10825-020-01483-9
14. Dréon J., Jeangros Q., Cattin J., Haschke J., Antognini L., Ballif C., Boccard M., "23.5%-efficient silicon heterojunction silicon solar cell using molybdenum oxide as hole-selective contact. Nano Energy". 2020 Apr 1, 70:104495. doi:10.1016/j.nanoen.2020. 104495.
15. Gao M., Chen D., Han B., Song W., Zhou M., Song X., Xu F., Zhao L., Li Y., Ma Z., "Bifunctional hybrid a-SiO x (Mo) layer for hole-selective and interface passivation of highly efficient MoO x/a-SiO x (Mo)/n-Si heterojunction photovoltaic device." ACS applied materials & interfaces, 2018 Jul 24;10(32):27454-64.doi:10.1021/acsami.8b07001.
16. Gao P., Zhenhai Y., "Dopant-Free and Carrier-Selective Heterocontacts for Silicon Solar Cells: Recent Advances and Perspectives," Photovoltaic Devices Adv. Sci. 5, April 2017, 1700547–1700567. DOI: 10.1002/advs.201700547
17. García-Hernansanz R., García-Hemme E., Montero D., Olea J., Del Prado A., Martil I., Voz C., Gerling LG., Puigdollers J., Alcubilla R., "Transport mechanisms in silicon heterojunction solar cells with molybdenum oxide as a hole transport layer. Solar energy materials and solar cells". 2018 Oct 1,185:61–5.doi:10.1016/j.solmat.2018.05.019.

18. García-Hernansanz R., Pérez-Zenteno F., Duarte-Cano S., Caudevilla D., Algaidy S., García-Hemme E., Olea J., Pastor D., Del Prado A., San Andrés E., Mártil I., "Inversion Charge Study in TMO Hole-Selective Contact-Based Solar Cells". IEEE Journal of Photovoltaics, 2023, July 21, p. 13(5), 656 – 662.**DOI:** 10.1109/JPHOTOV.2023.3295494
19. Geissbühler J, Werner J, Martin de Nicolas S, Barraud L, Hessler-Wyser A, Despeisse M, Nicolay S, Tomasi A, Niesen B, De Wolf S, Ballif C. 22.5% efficient silicon heterojunction solar cell with molybdenum oxide hole collector. Applied Physics Letters. 2015 Aug 24;107(8). https://doi.org/10.1063/1.4928747
20. Gerling LG., Voz C., Alcubilla R., and Puigdollers J., "Origin of passivation in hole-selective transition metal oxides for crystalline silicon heterojunction solar cells." Journal of Materials Research, 2017 Jan, 32(2):260–8. http://dx.doi.org/ 10.1557/jmr.2016.453
21. Gerling LG., Voz C., Alcubilla R., and Puigdollers J., "Origin of passivation in hole-selective transition metal oxides for crystalline silicon heterojunction solar cells." Journal of Materials Research, 2017 Jan, 32(2):260–8. http://dx.doi.org/ 10.1557/jmr.2016.453
22. Green M., Dunlop E., Hohl-Ebinger J., Yoshita M., Kopidakis N., and Hao X. Solar cell efficiency tables (version 57). Progress in photovoltaics: research and applications. 2021 Jan;29(1):3-15. doi: 10.1002/pip.3371
23. Green MA., "TThe passivated emitter and rear cell (PERC): From conception to mass production. Solar Energy Materials and Solar Cells". 2015 Dec 1;143:190–7. doi:10.1016/j.solmat.2015.06.055.
24. Greiner MT., Chai L., Helander MG., Tang WM., Lu ZH., "Transition metal oxide work functions: the influence of cation oxidation state and oxygen vacancies." Advanced Functional Materials. 2012 Nov 7, 22(21):4557–68. doi:10.1002/adfm.201200615
25. Greiner MT., Chai L., Helander MG., Tang WM., Lu ZH., "Metal/metal-oxide interfaces: how metal contacts affect the work function and band structure of MoO3". Advanced Functional Materials. 2013 Jan 14, 23(2):215-26. doi:10.1002/adfm.201200993
26. Hermle M., Feldmann F., Bivour M., Goldschmidt JC., Glunz SW., "Passivating contacts and tandem concepts: Approaches for the highest silicon-based solar cell efficiencies." Applied Physics Reviews. 2020 Jun 1;7(2). https://doi.org/10.1063/1.5139202
27. Hussain SQ., Mallem K., Khan MA., Khokhar MQ., Lee Y., Park J., Lee KS., Kim Y., Cho EC., Cho YH., Yi J., "Versatile hole carrier selective MoO x contact for high efficiency silicon heterojunction solar cells": A review. Transactions on Electrical and Electronic Materials, 2019 Feb 11;20:1-6.
28. Imran H., Abdolkader TM., Butt NZ., "Carrier-selective NiO/Si and TiO2/Si contacts for silicon heterojunction solar cells. IEEE Transactions on Electron Devices, 2016, July 18, 63(9):3584–90. **DOI:** 10.1109/TED.2016.2585523.
29. Kang D., Ko J., Lee C., Kim D., Lee H., Kang Y., and Lee HS., "Titanium oxide nanomaterials as an electron-selective contact in silicon solar cells for photovoltaic devices." Discover Nano. 2023 Mar 11, 18(1):39. | https://doi.org/10.1186/s11671-023-03803-x.
30. Khokhar MQ., Hussain SQ., Chowdhury S., Zahid MA., Pham DP., Jeong S., Kim S., Cho EC., Yi J., "High-efficiency hybrid solar cell with a nano-crystalline silicon oxide layer as an electron-selective contact. Energy Conversion and Management". 2022 Jan 15, 252:115033. https://doi.org/10.1016/j.enconman.2021.115033

31. Koswatta P., Boccard M., and Holman Z., “Carrier-selective contacts in silicon solar cells." In the 2015 IEEE 42nd photovoltaic specialist conference (PVSC), June 14, 2015 (pp. 1–4),. IEEE.DOI: 10.1109/PVSC.2015.7356143
32. Kumar M., Eun-Chel C., Maksym F., and Prodanov, “MoOx work function, interface structure, and thermal stability analysis of ITO/MoOx/a-Si(i) stacks for hole-selective silicon heterojunction solar cells," Applied Surface Science, July 2021, 553, 149552–149562. https://doi.org/10.1016/j.apsusc.2021.149552
33. Kumari J., Basumatary P., Gangwar MS., and Agarwal P., “Molybdenum oxide (MoO3-x) as an emitter layer in silicon-based heterojunction solar cells." Materials Today: Proceedings, 2021, Jan. 1, 39:1996–1999. https://doi.org/10.1016/j.matpr.2020.08.527
34. Lin H., Yang M., Ru X., Wang G., Yin S., Peng F., Hong C., Qu M., Lu J., Fang L., Han C., “Silicon heterojunction solar cells with up to 26.81% efficiency achieved by electrically optimised nanocrystalline-silicon hole contact layers," Nature Energy, 2023 Aug, 8(8):789–99.
35. Liu Y., Li Y., Wu Y., Yang G., “Mazzarella L, Procel-Moya P, Tamboli AC, Weber K, Boccard M, Isabella O, Yang X. High-efficiency silicon heterojunction solar cells: materials, devices, and applications." Materials Science and Engineering: R: Reports. 2020 Oct 1;142:100579. https://doi.org/10.1016/j.mser.2020.100579
36. Masmitja G., Ortega J., Puigdollers, Gerling L.G., “Interdigitated back-contacted crystalline silicon solar cells with low-temperature dopant-free selective contacts, J. Mater. Chem., January 2018, 63977–3985. DOI: 10.1039/C7TA11308K
37. Masmitjà, G., Ros, E., Almache-Hernández, R., Pusay, B., Martín, I., Voz, C., Saucedo, E., Puigdollers, J., and Ortega, P., “Interdigitated back-contacted crystalline silicon solar cells fully manufactured with atomic layer deposited selective contacts." Solar Energy Materials and Solar Cells, April 2022, 240, p. 111731. https://doi.org/10.1016/j.solmat.2022.11173113.
38. Markose k.k., Antony A., and Jayaraj M. K., "Factory of an Asymmetric Heterojunction Carrier Selective C-Si Solar Cell," AIP Conference Proceedings, November 2020, 2265, 030641. https://doi.org/10.1063/5.0016645
39. Martín I., López G., Garín M., Ros E., Ortega P., Voz C., Puigdollers J., “Hole selective contacts based on transition metal oxides for c-Ge thermophotovoltaic devices”. Solar Energy Materials and Solar Cells, 2023, March 1, 251:112156. https://doi.org/10.1016/j.solmat.2022.112156
40. Mehmood H., Nasser H., Tauqeer T., and Turan R. Simulation of a silicon heterostructure solar cell featuring dopant-free carrier-selective molybdenum oxide and titanium oxide contacts. Renewable energy. 2019 Dec 1;143:359-67. https://doi.org/10.1016/j.renene.2019.05.007
41. Mehmood H., Nasser H., Tauqeer T., and Turan R., “Numerical analysis of a dopant-free asymmetric silicon heterostructure solar cell with SiO2 as passivation layer." International Journal of Energy Research, 2020, October 25, 44(13):10739–53. https://doi.org/10.1002/er.572055
42. Melskens J., van de Loo BW., Macco B., Black LE., Smit S., Kessels WM., “Passivating contacts for crystalline silicon solar cells: From concepts and materials to prospects." IEEE Journal of Photovoltaics. 2018 Feb 14, 8(2):373–88. **DOI:** 10.1109/JPHOTOV.2018.279710656.
43. Messmer C., Bivour M., Schön J., and Hermle M., “Requirements for efficient hole extraction in transition silicon heterojunction solar cells." Journal of Applied Physics, 2018. Metal oxide-based Aug. 28, 124(8). doi:10. 1063/1.5045250

44. Michel J. Ibarra., Dréon J., Boccard M., Bullock J., and Macco B., “Carrier-selective contacts using metal compounds for crystalline silicon solar cells," Progress in Photovoltaics, February 2023, 31,380–413. https://doi.org/10.1002/pip.3552
45. Nayak M., Mandal S., Pandey A., Mudgal S., “Singh S., Komarala VK. Nickel oxide hole-selective heterocontact for silicon solar cells: role of SiOx interlayer on device performance”, Solar RRL. 2019 Nov, 3(11):1900261. DOI: 10.1002/solr.201900261
46. Nagamatsu K.A., Avasthi S., Sahasrabudhe G., “Titanium dioxide/silicon hole-blocking selective contact to enable doubleheterojunction crystalline silicon-based solar cell," Applied Physics Letters, March 2015, 106(12), 123906. https://doi.org/10.1063/1.4916540
47. Parashar PK., Komarala VK., “Sputter-deposited sub-stochiometric MoOx thin film as a hole-selective contact layer for silicon-based heterojunction devices." Thin Solid Films. 2019 Jul 31, 682:76–81. doi:10.1016/ j.tsf.2.019.05.004
48. Patwardhan S., Maurya S., Kumar, and Kavaipatti B., “Amorphous solar cells: free metal oxide-based carrier selective contacts to crystalline silicon solar cells," 35th European Photovoltaic Solar Energy Conference, September 2018, 657–659. https://www.researchgate.net/publication/337007871
49. Plakhotnyuk MM., Schüler N., Shkodin E., Vijayan RA., Masilamani S., Varadharajaperumal M., Crovetto A., Hansen O., “Surface passivation and carrier selectivity of the thermal-atomic-layer-deposited TiO2 on crystalline silicon." Japanese Journal of Applied Physics. 2017 Jul 26, 56(8S2):08MA11. https://doi.org/10.7567/JJAP.56.08MA11
50. Richter A., Müller R., Benick J., Feldmann F., Steinhauser B., Reichel C., Fell A., Bivour M., Hermle M., Glunz SW., “Design rules for high-efficiency both-sides-contacted silicon solar cells with balanced charge carrier transport and recombination losses." Nature Energy. 2021 Apr, 6(4):429–38. doi:10.1038/s41560-021-00805-w
51. Richter A., Benick J., Feldmann F., Fell A., Hermle M., Glunz SW., “n-Type Si solar cells with passivating electron contact: Identifying sources for efficiency limitations by wafer thickness and resistivity variation." Solar Energy Materials and Solar Cells, 2017 Dec 1, 173:96–105. doi:10.1016/J.SOLMAT.2017.05.042
52. Sagar R., Rao A., “Increasing the silicon solar cell efficiency with transition metal oxide nano-thin films as anti-reflection coatings." Materials Research Express. 2020 Jan 27, 7(1):016433. https://doi.org/10.1088/2053-1591/ab6ad5.
53. Sanyal S., Dutta S., Ju M., Mallem K., Panchanan S., Cho EC., Cho YH., and Yi J., “Hole Selective Contacts: A Brief Overview. Current Photovoltaic Research”. 2019 Mar, 7(1):9–14. https://doi.org/10.21218/CPR.2019.7.1.009
54. Schmidt J., Peibst R., and Brendel R., “Surface passivation of crystalline silicon solar cells: present and future." Solar Energy Materials and Solar Cells. 2018 Dec 1;187: 39–54.
55. Scirè D., Macaluso R., Mosca M., Casaletto MP., Isabella O., Zeman M., and Crupi I., “Density of state characterization of TiO2 films deposited by pulsed laser deposition for heterojunction solar cells. Nano Research”. 2022 May, 15(5):4048–57. https://doi.org/10.1007/s12274-021-3985-8.
56. Scirè D., Macaluso R., Mosca., Casaletto M.P., Isabella O., Zeman M., Crupiet I., “Transition metal oxides as selective contacts for c-Si solar cells”. Nano Research, December 2021, 11-5974/O4.
57. Shockley W., Queisser H., “Detailed balance limit of efficiency of p–n junction solar cells”, In Renewable Energy, 2018 Dec 14, (pp. Vol2_35-Vol2_54). Routledge. https://doi.org/10.1063/1.1736034.

58. Vijayan R.A., Masilamani S., Kailasam S., Shivam K., Deenadhayalan B., Varadharajaperumal M.. "Study of surface passivation and charge transport barriers in DASH solar cell. IEEE Journal of Photovoltaics". 2019 Jul 18, 9(5):1208-16. DOI: 10.1109/JPHOTOV.2019.2926624
59. Wang G., Zhang C., Sun H., "Understanding and design of efficient carrier-selective contacts for solar cells", AIP Advances 11, November 2021,11, 115026 , https://doi.org/10.1063/5.0063915
60. Wang Y., Zhang ST., Li L., Yang X., Lu L., Li D., "Dopant-free passivating contacts for crystalline silicon solar cells: Progress and prospects". EcoMat. 2023 Feb, 5(2):e12292.. https://doi.org/10.1002/eom2.12292
61. Wang Z., Li P., LiuHole Z., "Selective materials and device structures of heterojunction solar cells: Recent assessment and future trends", : APL Material. ,November 2019 ,7, 110701. https://doi.org/10.1063/1.5121327
62. Wenjie W., He J., Yan D., Samundsett C., Pheng S.P., Huang Z., Shen W., , Bullock J., Wan J., "21.3%-efficient n-type silicon solar cell with a full area rear TiOx/LiF/Al electron-selective contact", Solar Energy Materials & Solar Cells, March 2020, 206. 110291. https://doi.org/10.1016/j.solmat.2019.110291
63. Wong T.K.S., Pei K., "Double Hetero-junction Crystalline Silicon Solar Cells From Doped Silicon to Dopant-Free Passivating Contacts", Photonics, July 2022., 9(7) , 477-509. https://doi.org/10.3390/photonics9070477
64. Wu W., Lin W., Zhong S., Paviet-Salomon B., Despeisse M., Liang Z., Boccard M., Shen H., Ballif C., "22% efficient dopant-free interdigitated back contact silicon solar cells. InAIP Conference Proceedings 2018 Aug 10 (Vol. 1999, No. 1). AIP Publishing". doi:10.1063/1.5049288.
65. Yan D., Cuevas A., Phang SP., Wan Y., Macdonald D., "23% efficient p-type crystalline silicon solar cells with hole-selective passivating contacts based on physical vapor deposition of doped silicon films". Applied Physics Letters. 2018 Aug 6;113(6). https://doi.org/10.1063/1.5037610
66. Yang X., Bi Q., Ali H., Davis K., Schoenfeld WV., Weber K., "High-Performance TiO2-Based Electron-Selective Contacts for Crystalline Silicon Solar Cells". Advanced Materials (Deerfield Beach, Fla.). 2016 May 9, 28(28):5891-7. doi:10. 1002/adma.201600926.
67. Yoshikawa K., Kawasaki H., Yoshida W., "Silicon heterojunction solar cell with interdigitated back contacts for a photo-conversion efficiency over 26%", Nature Energy., March 2017,2, 17032-17040. DOI: 10.1038/nenergy.2017.32
68. Yu C., Xu S., Yao J., Han S., "Recent advances in and new perspectives on crystalline silicon solar cells with carrier-selective passivation contacts". Crystals. 2018 Nov 15, 8(11):430. doi:10.3390/cryst8110430
69. Zeng Y, Peng CW, Hong W, Wang S, Yu C, Zou S, Su X. Review on metallization approaches for high-efficiency silicon heterojunction solar cells. Transactions of Tianjin University. 2022 Oct;28(5):358-73.https://doi.org/10.1007/s12209-022-00336-9
70. Zhao Y., Procel P., Han C., Cao L., Yang G., Özkol E., Alcañiz A., Kovačević K., Limodio G., Santbergen R., Smets A., "Strategies for realizing high-efficiency silicon heterojunction solar cells" Solar Energy Materials and Solar Cells. 2023 Aug 15, 258:112413.DOI 10.1016/j.solmat.2023.112413